arXiv:1401.4414v1 [astro-ph.SR] 17 Jan 2014

Single Rotating Stars and the Formation of Bipolar Planetary Nebula

G. García-Segura

Instituto de Astronomía, Universidad Nacional Autónoma de Mexico, Km. 103 Carr. Tijuana-Ensenada, 22860, Ensenada, B. C., Mexico

ggs@astrosen.unam.mx

E. Villaver

Departamento de Física Teórica, Universidad Autónoma de Madrid, Cantoblanco, E-28049 Madrid, Spain

N. Langer

Argelander-Institut für Astronomie, Universität Bonn, D-53121 Bonn, Germany

S.-C. Yoon

Astronomy Program, Department of Physics and Astronomy, Seoul National University, Seoul, 151-747, Republic of Korea

and

A. Manchado[1,2]

Instituto de Astrofísica de Canarias, Via Láctea s/n, E-38200 La Laguna, Tenerife, Spain

Received _____; accepted _____

[1]Departamento de Astrofísica, Universidad de La Laguna, E-38206 La Laguna, Tenerife, Spain

[2]Consejo Superior de Investigaciones Científicas (CSIC), Spain

ABSTRACT

We have computed new stellar evolution models that include the effects of rotation and magnetic torques under different hypothesis. The goal is to test if a single star can sustain in the envelope the rotational velocities needed for the magneto hydrodynamical (MHD) simulations to shape bipolar Planetary Nebulae (PNe) when the high mass-loss rates take place. Stellar evolution models with main sequence masses of 2.5 and 5 $M_{\odot}$, and initial rotational velocities of 250 km s^{-1} have been followed all the way to the PNe formation phase. We find that stellar cores have to be spun down using magnetic torques in order to reproduce the rotation rates observed for white dwarfs. During the asymptotic giant branch phase and beyond, the magnetic braking of the core has a practically null effect in increasing the rotational velocity of the envelope since the stellar angular momentum is removed efficiently by the wind. We have, as well, tested best possible case scenarios in rather non-physical contexts to give enough angular momentum to the envelope. We find that we cannot get the envelope of a single star rotating at the speeds needed by the MHD simulations to form bipolar PNe. We conclude that single stellar rotators are unlikely to be the progenitors of bipolar PNe under the current MHD model paradigm.

Subject headings: Stars: Evolution —Stars: Rotation —Stars: Magnetic Fields —Stars: Asymptotic Giant Branch—Stars: White Dwarfs —ISM: Planetary Nebulae

1. INTRODUCTION

The overall details of the Planetary Nebulae (PNe) formation process are well understood since Kwok, Purton & Fitzgerald (1978) proposed that it takes place due to the collision of two winds: a slow one characteristic of the red giant phase and a faster one which is produced later, by the naked stellar nucleus (see also Kahn & West 1985; Balick 1987). Within this framework, PNe modeling efforts have mostly focused on the shaping process itself, since understanding the formation of the complex PNe morphologies remains one of the open questions in the field (see reviews by Pottasch 1984; Iben 1993; Balick & Frank 2002; Shaw 2012).

Models have achieved a good deal of sophistication in reproducing morphological features using the hydrodynamic collimation of the fast wind by an equatorial density enhancement mechanism first implemented by Icke (1988) and Icke et al. (1989). In these models, the density enhancement responsible for the collimation is built ad-hoc, as it is in the Mellema, Eulderink, & Icke (1991), Icke, Balick, & Frank (1992), Frank & Mellema (1994), and Dwarkadas, Chevalier, & Blondin (1996) models.

Nowadays that is clear that the aspherical slow-fast wind combination can reproduce most PNe morphologies, the problem is to understand how, or if, a single star can create the equatorial density asymmetries during the Asymptotic Giant Branch (AGB) phase. The greatest challenge is to generate asymmetric stellar outflows via the combination of the winds when they are constrained by stellar evolution.

The first attempt to link the density enhancement to the evolution of the star was made by García-Segura et al. (1999) by using a rotating star with (or without) a magnetized wind and the wind solution by Bjorkman and Cassinelli (1993). Matt et al. (2000) have also shown how an isolated AGB star can produce a dense equatorial disk using a dipole magnetic field on the surface of the star. A rotating star also provides a natural solution to

the problem of creating an AGB density enhancement with different degrees of collimation (García-Segura et al. 1999). Even the magnetic field topology is derived from what is expected in the solar wind, where the poloidal field lines connecting the outflowing wind to the solar surface are wound up due to the rotation of the Sun. So, it seems that, so far, most scenarios for single stars require the key ingredient of stellar rotation either as a starting point for the solution, as a consequence of the evolution, or just as a tool to generate the magnetic field.

The literature is abundant in calculations of massive star evolution with rotation and rotationally-induced processes (see e.g. Maeder & Meynet 2000; Heger et al. 2000) but very few computations for low-mass stars through the AGB phase, including the effect of rotation are available. Stellar evolution calculations for 1 to 3 $M_{\odot}$ stars with rotation have been computed to the early AGB phase by Suijs et al. (2008) to deduce the white dwarf (WD) angular momentum distribution. Recently, Prinja et al. (2012) have also presented the evolution of a 1.5 $M_{\odot}$ rotating star in their study of the PN NGC 6543. Both works arrived at the same general conclusion: that magnetic torques are needed to transfer the angular momentum from the rapidly spinning cores to the envelope in order to reproduced the observed rotational velocities of WDs (Kawaler 2004). In this paper, we focus on studying if the mechanism capable of reducing the spin of the core to match empirical values (a magnetic torque) is able to spin up the envelope to the values required by the MHD calculations.

We present new calculations of the evolution of 2.5 and 5 $M_{\odot}$ stars from the Zero-Age Main Sequence (ZAMS) to the post-AGB phase with rotation and magnetic torques using a realistic prescription for the mass-loss rate during the AGB phase. Motivated by the analytical estimates by García-Segura et al. (1999), the goal is to study whether we can obtain the rotation at the stellar surface needed to shape bipolar PN, by transferring under

different hypothesis, the angular momentum from the core.

The paper is organized as follows: the stellar evolutionary code is described in §2; the results of the calculations with and without magnetic torques are presented in §3 where we also provide the description of the models where the magnetic torques are switched on at selected times; a full discussion and the conclusions of the paper are provided in §4.

2. STELLAR MODELS

The stellar evolution calculations have been done using the Binary Evolution Code (BEC) (Petrovic et al. 2005; Yoon et al. 2006). BEC is a one dimensional hydrodynamic, stellar evolution code designed to evolve stellar models of single, and binary stars, which descends from the code for binary stars (Braun & Langer 1995) and from the code STERN (Langer 1991). The code includes diffusive mixing due to convection, semi-convection (Langer et al. 1985), and thermohaline mixing as in Wellstein et al. (2001). This code includes the effect of the centrifugal force on the stellar structure, and time-dependent chemical mixing and transport of angular momentum due to rotationally-induced instabilities (Heger et al. 2000). We also include chemical mixing and transport of angular momentum due to magnetic fields (Spruit 2002), as in Heger et al. (2005) and Petrovic et al. (2005). The rotation profile in the convection zone is self-consistently calculated by solving the diffusion equation within the code.

We calculate the evolution of stars with initial stellar masses of 2.5 and $5M_{\odot}$ and solar metalicity. Two main reasons motivate the choice of the initial progenitor masses. First, the single star hypothesis for the formation of bipolar PNe has been suggesting higher mass stellar progenitor for this morphological class as indicated by their chemical abundances (see e.g. Stanghellini et al. 2006; Manchado et al. 2000), and their closer distribution to the

galactic plane (Corradi & Schwarz 1995). Second, we aim to constrain the mechanism for the most favorable scenario and faster rotators are found among the main sequence (MS) stars with the higher masses within the PNe progenitor mass range.

We have adopted an initial, representative equatorial rotation velocity of 250 km s^{-1} at the ZAMS (Fukuda 1982). The mass-loss rate used is the one by Reimers (1975) for the Red Giant phase with an $\eta = 0.5$ parameter and that by Vassiliadis & Wood (1993) for the AGB phase. For the 2.5 $M_\odot$ star we have computed the evolution from the ZAMS to the post-AGB phase to the point were the remaining stellar mass is 0.67 $M_\odot$. This star loses 1.83 $M_\odot$ through the mass-loss at the AGB thermally pulsating phase. The $5M_\odot$ model calculation is stopped after 19 thermal pulses beyond which the CO core angular momentum does not change significantly (see also Suijs et al. 2008).

3. RESULTS

The evolution of a ZAMS 2.5 $M_\odot$ star in the Hertzsprung-Russell (HR)-diagram is shown in Figure 1. The track shows how the star undergoes the major evolutionary phases, MS, Red Giant Branch (RGB) and AGB. It also shows the characteristic modulations associated to the thermal-pulses taking place in the stellar interior at the end of the AGB phase. As mentioned before, the mass-loss rate mode has been changed between the RGB and AGB phases from the Reimers prescription to the Vassiliadis & Wood (1993) parameterization which has a dependency with the pulsational period of the star which in turn translates into a period-mass-radius relation. The stellar evolution is followed well into the post-AGB phase (for the meaning of the marks in the plot see §3.1). The model in Figure 1 has been computed using magnetic torques and with an initial rotational velocity of 250 km s^{-1} . The evolution of the model without magnetic torques is very similar. The only significative difference is that the modulations associated to the thermal pulses at the

tip of the AGB occur at slightly different locations in the HR diagram.

The evolution of the surface equatorial rotational velocity is presented in Figure 2 for the 2.5 $M_\odot$ star and the non-magnetic case. The top panels show the evolution up to the early thermal pulsing (TP) AGB phase and the bottom panels the evolution of the rotational velocity until the end of the calculation when the star is well into the post-AGB phase. Note the difference in scale between the top and the bottom panels in the figures.

Along the MS evolution of the star, the density increases in the stellar core leading to a more efficient nuclear burning, and to a tiny increase in the stellar radius. This causes a decrease in the rotational velocity along in the first $\approx 5 \times 10^8$ yr of the evolution (the largest radius reached at the MS is 3.8 $R_\odot$) as seen in the top panel of Figure 2.

The point of H-core burning exhaustion induces a small peak in the surface rotational velocity which is immediately followed by an abrupt drop consequence of the expansion in the radius along the RGB (up to 25 $R_\odot$). During the He-core burning phase the surface rotational velocity remain at a value of 15 km s^{-1} with the stellar radius during this phase remaining at a nominal value of 8.4 $R_\odot$. The evolution during the AGB phase begins past 7.4×10^8 yr and it is characterized by stellar expansion, heavy mass-loss rates, and thermal-pulses. The multiple peaks in the bottom of Figure 2 are associated to the increase in radius experienced by the star in the aftermath of the pulses. The surface rotational velocity at the last point shown at the bottom of Figure 2 (that of a post-AGB star with 6400 K) is almost zero.

We find that when the 2.5 $M_\odot$ star, evolving without magnetic field-induced internal angular momentum transport, reaches the post-AGB phase, it has lost most of its angular momentum and its surface rotation velocity is 9.7 $\times 10^{-6}$ km s^{-1} . Similar results are obtained for the 5 $M_\odot$ star which reaches a surface rotation velocity of 10^{-6} km s^{-1} at the end of the AGB phase.

Figure 3 shows the evolution of a 2.5 $M_\odot$ star including the effects of angular momentum transport due to magnetic fields (see Spruit 2002). The overall behavior of the surface equatorial rotational velocity is similar to the non-magnetic case shown before. Small differences are found for instance in the velocity peak reached at the end of the MS, or in the smaller velocity in the surface at the beginning of the AGB, and are due to the more efficient transport of angular momentum between the core and the envelope (Heger & Langer 1998). The slightly different evolutionary timescales between the magnetic and non-magnetic models are caused by the same effect.

In this calculation using magnetic torques the surface rotational velocity is almost zero, 8.4 $\times 10^{-6}$ km s^{-1} , at the post-AGB phase when the star has reached a temperature of 6400 K. The magnetic 5 $M_\odot$ star reaches a surface rotation velocity at the end of the computed evolution of 4 $\times 10^{-6}$ km s^{-1} .

In Figure 4 we show snapshots of the distribution of the rotational velocities within the stellar structure taken at key evolutionary times. The non-magnetic model is plotted on the left, and the magnetic model in the right panels. From top to bottom are shown the ZAMS, the end of the MS, RGB, He-core burning phase, and the post-AGB phase when the star has reached a temperature of 6400 K. The top panels, taken at the ZAMS, represent the initial conditions for both models, a constant angular velocity with a solid body rotation of $v_{surf} = 250$ km s^{-1} .

If we focus in the left panels showing the non-magnetic model, we see that at the end of H-core burning, the recently formed He-core has been slightly spun up by contraction (angular momentum conservation) to 40 km s^{-1} while the surface slows down by the expansion of the envelope. Note that the radiative envelope still rotates as a solid body. By the end of the RGB phase (H-shell burning), the third panel from the top shows that the dense He-core has been spun up to 150 km s^{-1} by a much larger contraction, while the

expansion of the envelope to a radius of 25 $R_\odot$ has slowed down the surface velocity to a value of ≈ 5 km s^{-1} . By the end of the He-core burning, fourth panel, the core is slowed down by redistribution of angular momentum. The core rotates at 55 km s^{-1} , while the surface is rotating at only 10 km s^{-1} .

By the time the star reaches the AGB phase the contraction of the still forming CO core produces a spin-up at the center, while the large expansion of the convective envelope, up to 500 $R_\odot$, slows down completely the stellar surface. This results in a star that at the post-AGB phase has a fast rotating CO degenerate core that will finally end up as a very fast (150 km s^{-1}) spinning WD.

The magnetic model in the right panels of Figure 4 show the action of magnetic torques between core and envelope operating along the whole evolution. This is evident at the end of the RGB phase, where the star as a whole has completely slow down its rotation to values under 4 km s^{-1} . Note instead the core speed of 150 km s^{-1} of the model without magnetic torques. At the post-AGB phase, the core only rotates at 5 km s^{-1} . This value of the rotational velocity match better those obtained through asterosismological observations of ZZ Ceti stars (Bradley 1998, 2001;Dolez 2006; Handler 2001, Handler et al. 2002; Kepler et al. 1995; Kleinmann et al. 1998; Winget et al. 1994). As already pointed out by Suijs et al. (2008), magnetic torques are required to reproduce the slow rotation rates observed for WDs.

3.1. Hypothetical Cases

Let us assume that we have a 2.5 $M_\odot$ non-magnetic model up to the AGB phase and that the angular momentum of the core can be transported to the envelope at the end of the evolution. This will be along the lines of the more “optimistic” case discussed in

García-Segura et al. (1999) for the formation of bipolar PNe (see below). The CO core has a mass of 0.656 $M_\odot$ and it is rotating at 150 km s^{-1} . It is logical then to assume that an important change in the surface rotation will occur once the angular momentum is transported outwards. To analyze this hypothetical scheme, we have explored three cases computed without magnetic braking until the stellar mass reaches 2.45, 1.85, and 0.674 $M_\odot$ respectively. At which point the magnetic braking is switched on. These models are labelled A, B and C respectively. The location in the HR diagram where the magnetic braking is turned on is marked in Figure 1 (see also Figure 5). Physically these models correspond to the beginning of the thermal pulses (model A), to the next to last thermal pulse (model B), and to a few thousand years before the PNe formation.

In Figure 5 we show the evolution of the helium burning luminosity as a function of the stellar mass for the model without magnetic braking. It is important to note that more than half of the stellar mass is lost in just the last two thermal pulses (see also Vassiliadis & Wood 1993), and that there are no meaningful differences regarding the mass-loss between the magnetic and non-magnetic models.

Figure 6 shows the rotational structure of the star at the post-AGB phase, when the star is in the blueward evolution and has reached a temperature of 6400 K, just a few thousand years before the PN becomes ionized. The CO core of model A rotates at 6 km s^{-1} which agrees with the typical rotation velocities observed in WDs. The cores of models B and C rotate at 17 and 80 km s^{-1} respectively, values above the observational limit of 10 km s^{-1} (Suijs et al. 2008) .

The late turn on of the magnetic braking used in models A and B has no appreciable effect on the rotational velocities reached on the surface of the star. Only for model C we find a noticeable increase of the surface rotation. However, model C rotates at only 1.8 km s^{-1} by the time the star reaches the post-AGB phase (at 6400 K), while the escape

velocity has increased up to ~ 50 km s^{-1} . A faster rotation than that reached would be required in order to produce asymmetries by the wind compressed model (Bjorkman & Cassinelli 93; Ignace et al. 1996).

It is interesting to note in Figure 5 that the Helium production of energy during the thermal pulses is increased up to 7 orders of magnitude but is never turned off completely during the inter-pulse phases. The fact that energy production in the helium shell is never completely switched off in the evolution rules out the "optimistic" scenario proposed by García-Segura et al. (1999). The consequence is that an entropy barrier always remains in the inter-pulse phase in the non-magnetic model.

An entropy barrier, i.e., a positive entropy gradient, is formed, e.g., at the location of a nuclear burning shell due to the production of heat. In a chemically homogeneous situation, this implies a stabilizing effect (buoyancy) which is proportional to the entropy gradient (Kippenhahn & Weigert 1990), implying that the larger the entropy gradient, the more stable is the stratification. Any radial gas motion present in this case will be damped, giving rise to a dynamically stable configuration (*Schwarzschild criterion*). If there is a chemical gradient present in the plasma (μ-barrier) its effect is added to the effects of the entropy gradient. As a consequence, a negative μ-gradient, such as the one present in our our calculations (see also Langer et al. 1999; Heger et al. 2000) of a CO-core surrounded by an envelope of H and He is highly stabilizing (*Ledoux criterion*). Note that convective mixing occurs when the entropy is rather constant, i.e., in adiabatic conditions, or when lower-entropy gas lies above higher-entropy gas, since the adiabatic gradient is normally positive.

The "optimistic case" involves an scenario in which the He-core evolves decoupled from the envelope and retains its angular momentum, i.e., the entropy barrier of a nuclear burning shell prevents that angular momentum can leak out of the core. When the star

move to the TP-AGB phase, the H and He burning shells are alternatively switched on and off. Thus the plausible barriers vanish periodically and core-envelope angular momentum exchange could occur during this stage. But, as Figure 5 shows, there is a stable minimum burning configuration that prevents the total leak to the envelope of the core angular momentum.

The effect of the drain of some angular momentum out through the H-and He-shells during the TP-AGB is visible in Figure 7 on the little spikes in the $j_s(t)$ curve, where is shown the specific angular momentum of the surface layers calculated as $j_s = R \times v_{surf}$. These small leaks are just buried under the stronger effect of the heavy winds, especially towards the end of the evolution when most of the mass is carried away from the star.

Figure 8 shows the evolution of the stellar radius and the surface equatorial rotational velocity for the model without magnetic torques. It is shown only the interval from the last three thermal pulses to the post-AGB phase when the star reaches a temperature of 6400 K. Note that the stellar material that will form the optical ionized nebula is the material ejected only during the last pulse (see Villaver et al. 2002) and at this time the rotation velocity in the stellar surface is of the order of $\sim 10^2$ cm s^{-1} .

4. DISCUSSION AND CONCLUSIONS

We have conducted a series of stellar evolutionary calculations in order to test if we can obtain, from a rotating ZAMS star, the velocities in the stellar surface at the tip of the AGB evolution that MHD models need to form bipolar PNe. Rotational speeds above 80 % of the critical rotation value are needed (the closer to critical rotation the better, where the Ω limit or break up speed is achieved; see García-Segura et al. 1999; Ignace et al. 1996). The critical rotation is defined as, $v_{\rm crit} = \sqrt{GM(1-\Gamma)/R}$ where, G is the gravitational

constant, M and R the stellar mass and radius. The term $\Gamma = L/L_{\rm edd}$ is just the ratio between L the stellar luminosity and $L_{\rm edd}$ the Eddington luminosity. For AGB winds, Γ should be close to unity by definition, so, one would expect that the critical velocity should be close to zero or approaching it. However, since the sound speed at the surface of an AGB star is of the order of ~ 1 km s^{-1} , values below that for the rotation will not have any impact in the wind compression mechanism (Bjorkman & Cassinelli 93; Ignace et al. 1996). We are obtaining from the stellar evolutionary calculations, rotational speeds in the surface at the end of the AGB of at most 1×10^{-5} km s^{-1} which are too small and are independent on whether we include or not magnetic field induced angular momentum transport in the calculations. Note that the value given from model C of 1.8 km s^{-1} is for the post-AGB phase when the star has 6400 K. At the TP-AGB phase, model C also has 1×10^{-5} km s^{-1} . It is interesting to mention that the model by Dorfi & Höfner (1996) also require velocities from 3 to 7 km s^{-1} to become efficient.

Based on our calculations, we can now argue against the formation of bipolar nebulae by the effects of rotation from single stars. For that, we compare the initial angular momentum with the one obtained at the end of the AGB phase. The initial total angular momentum of the 2.5 M$_\odot$ star is $J_{\rm ZAMS} = 7.095 \times 10^{50}$ g cm^2 s^{-1} . At the end of the AGB, when $t = 7.80637 \times 10^8$ yr (see Figure 8), the values for the radius and rotational velocity are $R = 463$ R$_\odot$ and $v_{surf} = 296$ cm s^{-1} . That time represents the moment the star reaches the largest radius just before the last thermal pulse and when the mass-loss rate is the largest for a longer period of time. Integrating the stellar structure, we then obtain a total angular momentum of $J_{\rm AGB} = 5.667 \times 10^{48}$ g cm^2 s^{-1} . The decrease of two orders of magnitude, i.e., a factor of 125, is due to mass loss (Heger & Langer 1998). This angular momentum can be split in $J_{\rm core} = 4.018 \times 10^{48}$ g cm^2 s^{-1} and $J_{\rm env} = 1.649 \times 10^{48}$ g cm^2 s^{-1} , for the core and the envelope respectively, where the CO core has a mass of $M_{\rm core} = 0.656$ M$_\odot$ and the envelope $M_{\rm env} = 0.352$ M$_\odot$, being the total mass $M_{\rm tot} = 1.008$ M$_\odot$.

The rotational velocity at the end of the AGB phase is 296 cm s^{-1} , and at least 2 km s^{-1} are needed to have a mechanism capable of producing asymmetries by the AGB slow wind. This implies that we need to achieve a rotational velocity a factor of 676 larger. Assuming rigid rotation because of convection, increasing the surface velocity by this factor implies to increase in the same factor the total angular momentum of the envelope. This gives a new value for the "ideal" envelope angular momentum of $J_{\rm ideal} = 1.115 \times 10^{51}$ g cm^2 s^{-1} , which is a factor of 1.57 larger than the ZAMS angular momentum of the whole star ($J_{\rm ZAMS}$). This is impossible to achieve for a single, isolated star, since the angular momentum at any given time cannot be larger than the initial one. Note also that achieving this angular momentum for the envelope at the end of the AGB would require the star at the ZAMS to be rotating at velocities orders of magnitude larger than the break up limit which for this stars is of the order of 300 km s^{-1} (Collins 1974).

We find that the amount of angular momentum needed to operate a MHD mechanism at the stellar surface cannot be provided by the star itself. However, it could be easily injected externally by a stellar or substellar companion. Just a 6 jupiter mass planet at an orbital distance of 5 AU has this amount of angular momentum and it has been shown can be easily engulfed into the stellar surface by tidal forces reaching far beyond the stellar radius (Villaver & Livio 2007, 2009; Mustill & Villaver 2012). The effects on the stellar rotation of binaries in general will be the subject of a future article.

We find that the inclusion of angular momentum transport through magnetic fields, and the coupling between the rapidly rotating core and the slowly rotating envelope produce the right amount of core spin down (see Heger et al. 2005; Petrovic 2005) to explain the observed rotational velocities of WDs. While this conclusion has been reached before (Suijs et al. 2008), this is the first time that a rotating stellar evolutionary model is computed with the inclusion of realistic AGB mass-loss rates that account for the

modulations associated with the thermal-pulses. We find that magnetic field induced angular momentum transport is needed to slow down the CO cores and that the same process is not capable of spinning up the envelopes. Even if we make the exercise to compute what would be the maximum rotational velocity of the star in the ideal situation where all the momentum from the core could be transported out to the envelope at $t = 7.80637 \times 10^8$ yr ($J_{\rm env}^{\rm max} = J_{\rm core} + J_{\rm env} = 5.667 \times 10^{48}$ g cm^2 s^{-1}) we can only increase the rotational velocity from 296 up to 1017 cm s^{-1} . We have to conclude that the remaining momentum in the core is not enough to speed enough the envelope.

We have also carried out a number of ad-hoc experiments where the magnetic torques are turned-on at the end of the evolution of the star, when the core is still rotating fast. In none of the three cases considered, selected to provide the best possible conditions to transfer angular momentum to the stellar surface, we can get the envelope rotating. These experiments just strengthen the conclusions of this paper, we cannot get the envelope rotating and the core slowed down even under the best case scenario provided by the physics of the problem.

Note that non-magnetic rotational transport processes have been found to be negligible for low-mass stars to slow down the stellar core (Langer et al. 1999; Palacios et al. 2003; 2006). Other mechanisms besides magnetic torques might exit (see Talon & Charbonnel 2005), such as angular momentum transfer through internal gravity waves (Zahn et al. 1997) but will not alleviate the problem we are having to speed up the envelope, as we have shown above.

The use of the particular prescription of Vassiliadis and Wood (1993) for the mass-loss rate is not expected to affect our main conclusion. First, for the magnetic case the core has already slowed down on the RGB so the differences in the evolution of the star imposed by a different mass-loss prescription will not be noticeable at all in the rotational speeds of the

envelope. Second, although the non-magnetic case is more susceptible to be affected by the adopted mass-loss rates we have shown that this model is not realistic since it leads to the formation of a fast rotating CO core which is not supported by observations.

Note, nonetheless that the Vassiliadis and Wood (1993) mass-loss parameterization is the most widely used for this phase, however, it has its limitations. In particular, it restrict the maximum amount of mass-loss to the radiation pressure limit value, while it has been observed that dust driven winds could exceed this limit by a factor of ~ 2 (Knapp 1986; Wood et al. 1992; Whitelock, Feast & Catchpole 1991). Larger AGB radius would be expected if higher mass-loss rates are reached during the thermal-pulses leading to an even more pronounced decrease of the rotational speeds of the envelope. Smaller mass-loss rates would have the opposite effect on the radius but they would delay the evolution of the star.

The explicit assumption within this work is that to develop a bipolar outflow we require rotational speeds that allow the formation of a wind-compressed disk (Bjorkman & Cassinelli 1993). However, bipolar flows can be formed, in principle, by other mechanisms such as the magnetic bomb discussed by Matt et al. (2006) in which the wind can be effectively collimated by a strong magnetic field tied to a star eliminating the need of an external disk. In the Matt et al. (2006) simulations at $t = 0$, the core begins rotating at a constant rate of at least 10% of the escape speed. Using a representative core mass and radius in our models ($R_{\rm core} = 10^9$ cm and $M_{\rm core} = 0.656 {\rm M}_\odot$) we obtain a escape velocity of 4172 km s^{-1} which would require in the Matt et al. (2006) model an initial core rotational velocity of 417 km s^{-1} . This core rotational speed is a factor 2.78 larger than what we obtain in the best case scenario, the non-magnetic model (~ 150 km s^{-1}), and a factor 83 larger than that obtained for the magnetic model, ~ 5 km s^{-1} . So even a purely magnetic collimation mechanism for the wind seems to require core rotational speeds larger than those that a single rotating star can produce.

A different possibility is that suggested by Frank (1995) and Soker (1998) in which the formation of magnetic spots at the surface of AGB stars is responsible of the formation of an equatorial density enhancement. In this scenario, turbulent dynamos of the $\alpha^2\Omega$ type (Soker & Zoabi 2002) should generate such magnetic fields since the stellar rotation is very small (~ 300 cm s^{-1} in our case, which is translated into $\sim 10^{-4}\omega_{\rm Kep}$). Dust should be efficiently formed above the cold spots giving rise to an enhancement on the mass loss rate. However, as discussed by the authors, these spots have to be formed preferently close to the equator and this mechanism would work only for the formation of elliptical nebulae given that the density ratio between pole a equator is smaller than 2.

Finally, concerning just single stars, the only mechanism available in the literature left to produce an equatorial density enhancement in the slow, AGB stellar wind, would be the one studied by Matt et al. (2000). In this study, a non-rotating AGB star produces a dipole magnetic field that enforces a wind compression towards the equator. Rotation, convection or a combination of both is necessary to produce a dynamo able to generate a magnetic field (Ω, α or $\alpha - \Omega$ dynamos respectively). Since we have computed in this paper that rotation is negligible in AGB stellar envelopes, convection would be the only relevant mechanism. All AGB stars have convective envelopes, independently of its stellar mass. But, from observations, bipolar PNe are not formed around all stars. If a dipole magnetic field is the mechanism at work for single stars to form bipolar planetary nebulae we would require the presence of an extra-parameter in the models to understand better the relatively small percentage of bipolar PNe formed.

AGB wind asphericities could result as well from the interaction of the AGB star with a binary companion (Livio 1993; Soker 1997; Nordhaus & Blackman 2006; de Marco 2009; de Marco et al. 2013). The interaction could involve the spin-up of the envelope by tidal forces, Roche lobe overflows, and common envelope evolution. Binary interactions are

beyond the scope of the present work and it will be the subject of a future paper.

In conclusion, according to state-of-the-art stellar evolution calculations of low-intermediate masses which includes the effects of rotation and stellar magnetic fields, single stellar rotators cannot be the precursors of bipolar planetary nebulae under the current MHD models requiring toroidal fields. If dipolar magnetic fields are invoked, extra-ingredients are needed, besides the presence of the magnetic field, to explain why bipolar PNe are not ubiquitously formed around all stellar masses.

G.G.-S. is partially supported by CONACyT grant 178253 and DGAPA grant IN100410. E.V. work was supported by the Spanish Ministerio de Ciencia e Innovación (MICINN), Plan Nacional de Astronomía y Astrofísica, under grant AYA2010-20630 and by the Marie Curie program under grant FP7-People-RG268111. A.M. acknowledge support for this work provided by the Spanish Ministry of Economy and Competitiveness under grant AYA-2011-27754. We would like to thank our anonymous referee for his valuable comments which improved the presentation of the paper

REFERENCES

Balick, B. 1987, AJ, 94, 671

Balick, B., & Frank, A. 2002, ARA&A, 40, 439

Bjorkman, J. E. & Cassinelli, J. P. 1993, ApJ, 409, 429

Bradley, P. A. 1998, ApJS, 116, 307

Bradley, P. A. 2001, ApJ, 552, 326

Braun, H. & Langer, N. 1995, in IAU Symposium 163, 305

Collins II, G. W. 1974, ApJ, 191, 157

Corradi, R. L. M. & Schwarz, H. E. 1995, A&A, 293, 871

De Marco, O. 2009, PASP, 121, 316

De Marco, O., Passy, J.-C., Frew, D. J., Moe, M., Jacoby, G. H. 2013, MNRAS, 428, 2118

Dolez, N., Vauclair, G., Kleinman, S. J., et al. 2006, A&A, 446, 237

Dorfi, E. A., & Höfner, S. 1996, A&A, 313, 605

Dwarkadas, V. V., Chevalier, R. A. & Blondin, J.M. 1996, ApJ, 457, 773

Frank, A. 1995, AJ, 110, 2457

Frank, A. & Mellema, G. 1994, A&A, 289, 937

Fukuda, I. 1982, PASP, 94, 271

García-Segura, G., Langer, N., Różyczka, M., & Franco, J. 1999, ApJ, 517, 767

Handler, G. 2001, MNRAS, 323, L43

Handler, G., Romero-Colmenero, E., & Montgomery, M. H. 2002, MNRAS, 335, 399

Heger, A., Langer, N., & Woosley, S. E. 2000, A&A, 2000, ApJ, 528, 368

Heger A., Langer N., 1998, A&A, 334, 210

Heger, A., Woosley, S. E., & Spruit, H. C. 2005, ApJ, 626, 350

Iben, I. Jr. 1993, in IAU Symp. No 155 "Planetary Nebulae", ed. R. Weinberger and A. Acker, (Kluwer Academic Publishers, Dordrecht), 587

Icke, V. 1988, A&A, 202, 177

Icke, V., Preston, H. L. & Balick, B. 1989, AJ, 97, 462

Icke, V., Balick, B. & Frank, A. 1992, A&A, 253, 224

Ignace, R., Cassinelli, J. P., & Bjorkman, J. E. 1996, ApJ, 459, 671

Kahn, F. D., & West, K. A. 1985, MNRAS, 212, 837

Kawaler, S. D. 2004, in IAU Symp. No 215, 561

Kepler, S. O., Giovannini, O., Wood, M. A., et al. 1995, ApJ, 447, 874

Kippenhahn, R., & Weigert, A. 1990, "Stellar Structure and Evolution", Springer-Verlag Berlin, Heildelberg, ISBN 0-387-50211-4

Kleinman, S. J., Nather, R. E., Winget, D. E., et al. 1998, ApJ, 495, 424

Knapp, G. R. 1986, ApJ, 311, 731

Kwok, S., Purton, C. R. & Fitzgerald, P. M. 1978, ApJ, 219, L125

Langer, N. 1991, A&A, 252, 669

Langer, N., El Eid, M. F., & Fricke, K. J. 1985, A&A, 145, 179

Langer, N., Heger, A., Wellstein, S., & Herwig, F. 1999, A&A, 346, L37

Livio, M. 1993, in IAU Symp. No 155 "Planetary Nebulae", ed. R. Weinberger and A. Acker, (Kluwer Academic Publishers, Dordrecht), 279

Maeder, A., & Meynet, G. 2000, ARA&A, 38, 143

Manchado, A., Villaver, E., Stanghellini, L., & Guerrero, M. A. 2000, ASP Conference Series, 199, 17

Matt, S., Balick, B., Winglee, R., & Goodson, A. 2000, ApJ, 545, 965

Matt, S., Frank, A., & Blackman, E. G. 2006, ApJ, 647, L45

Mellema, G., Eulderink, F. & Icke, V. 1991, A&A, 252, 718

Mustill, A. J., & Villaver, E. 2012, ApJ, 761, 121

Nordhaus, J., & Blackman, E. G. 2006, MNRAS, 370, 2004

Palacios, A., Talon, S., Charbonnel, C., & Forestini, M. 2003, A&A, 399, 603

Palacios, A., Charbonnel, C., Talon, S., & Siess, L. 2006, A&A, 453, 261

Petrovic, J., Langer, N., Yoon, S.-C., & Heger, A. 2005, A&A, 435, 247

Pottasch, S. R. 1984, "Planetary Nebulae. A Study of Late Stages of Stellar Evolution", (D. Reidel Publishing Company, Dordrecht)

Prinja, R. K., Massa, D. L., & Cantiello, M. 2012, ApJ, 759, L28

Reimers, D. 1975, Mem. Soc. Liege, 8, 369

Shaw, R. A. 2012, in IAU Symp. No 283, 156

Soker, N. 1997, ApJS, 112, 487

Soker, N. 1998, MNRAS, 299, 1242

Soker, N., & Zoabi, E. 2002, MNRAS, 329, 204

Spruit, H. C. 2002, A&A, 381, 923

Stanghellini, L., Guerrero, M. A., Cuuha, K., Manchado, A., & Villaver, E. 2006, ApJ, 651, 898

Suijs, M. P. L., Langer, N., Poelarends, A.-J., Yoon, S.-C., Heger, A., Herwig, F. 2008, A&A, 481, L87

Talon, S. & Charbonnel, C. 2005, A&A, 440 , 981

Vassiliadis, E., & Wood, P. R. 1993, ApJ, 413, 641

Villaver, E., Manchado, A., & García-Segura, G. 2002, ApJ, 581, 1204

Villaver, E., & Livio, M. 2007, ApJ, 661, 1192

Villaver, E., & Livio, M. 2009, ApJ, 705, L81

Wellstein, S., Langer, N., & Braun, H. 2001, A&A, 369, 939

Whitelock, P., Feast, M., & Catchpole, R. 1991, MNRAS, 248, 276

Winget, D. E., Nather, R. E., & Clemens, J. C. 1994, ApJ, 430, 839

Wood, P. R., Whiteloak, J. B., Hughes, J. M. G., Bessell, M. S., Gadner, F. F., & Hyland, A. R. 1992, ApJ, 397, 552

Yoon, S.-C., Langer, N., & Norman, C. 2006, A&A, 460, 199

Zahn, J.-P., Brun, A. S., & Mathis, S. 2007, A&A, 474, 145

This manuscript was prepared with the AAS LaTeX macros v5.2.

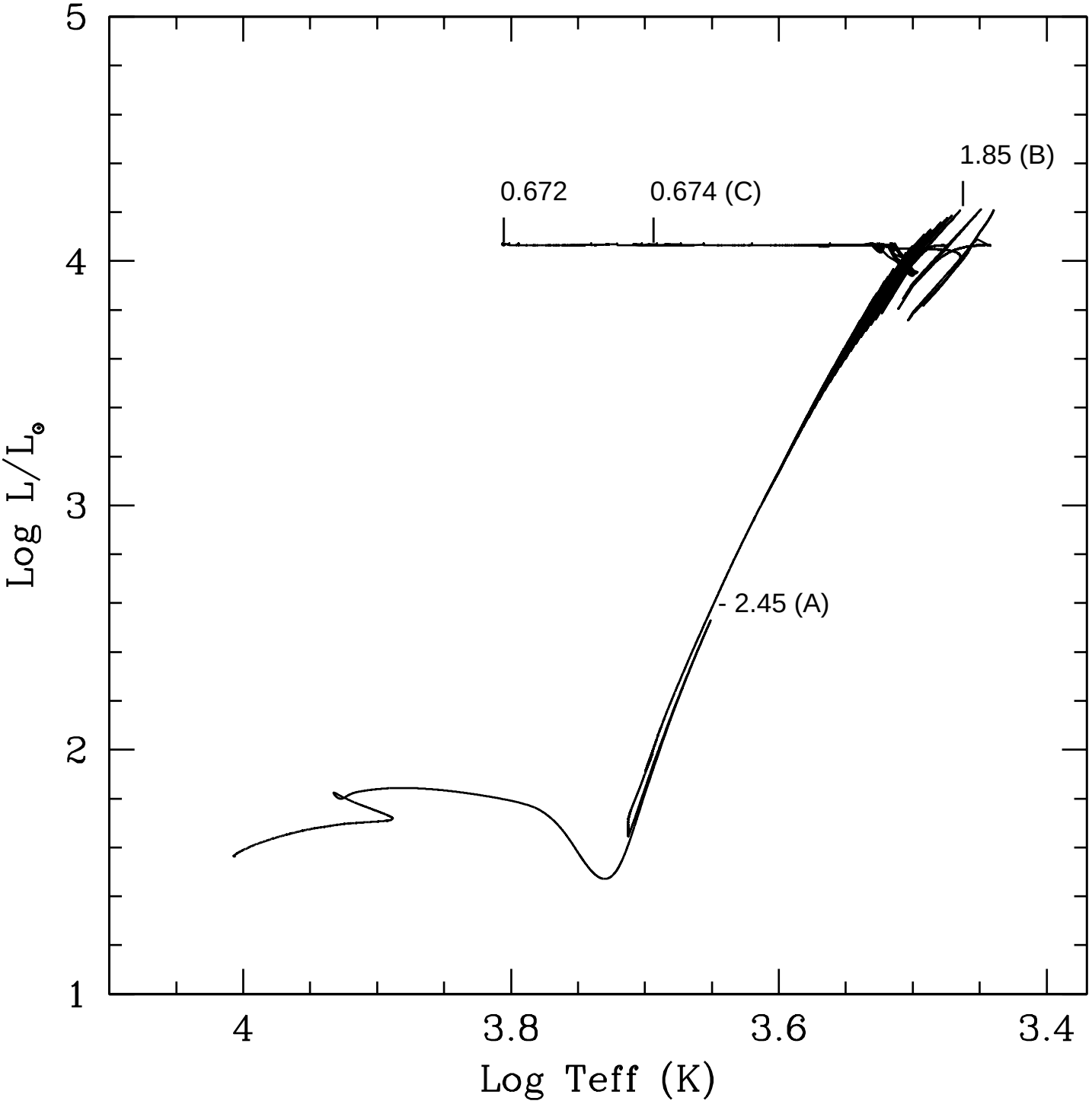

Fig. 1.— Evolutionary track of the magnetic 2.5 $M_\odot$ star on the HR diagram. The ZAMS rotational velocity assumed for this model is 250 km s^{-1} .

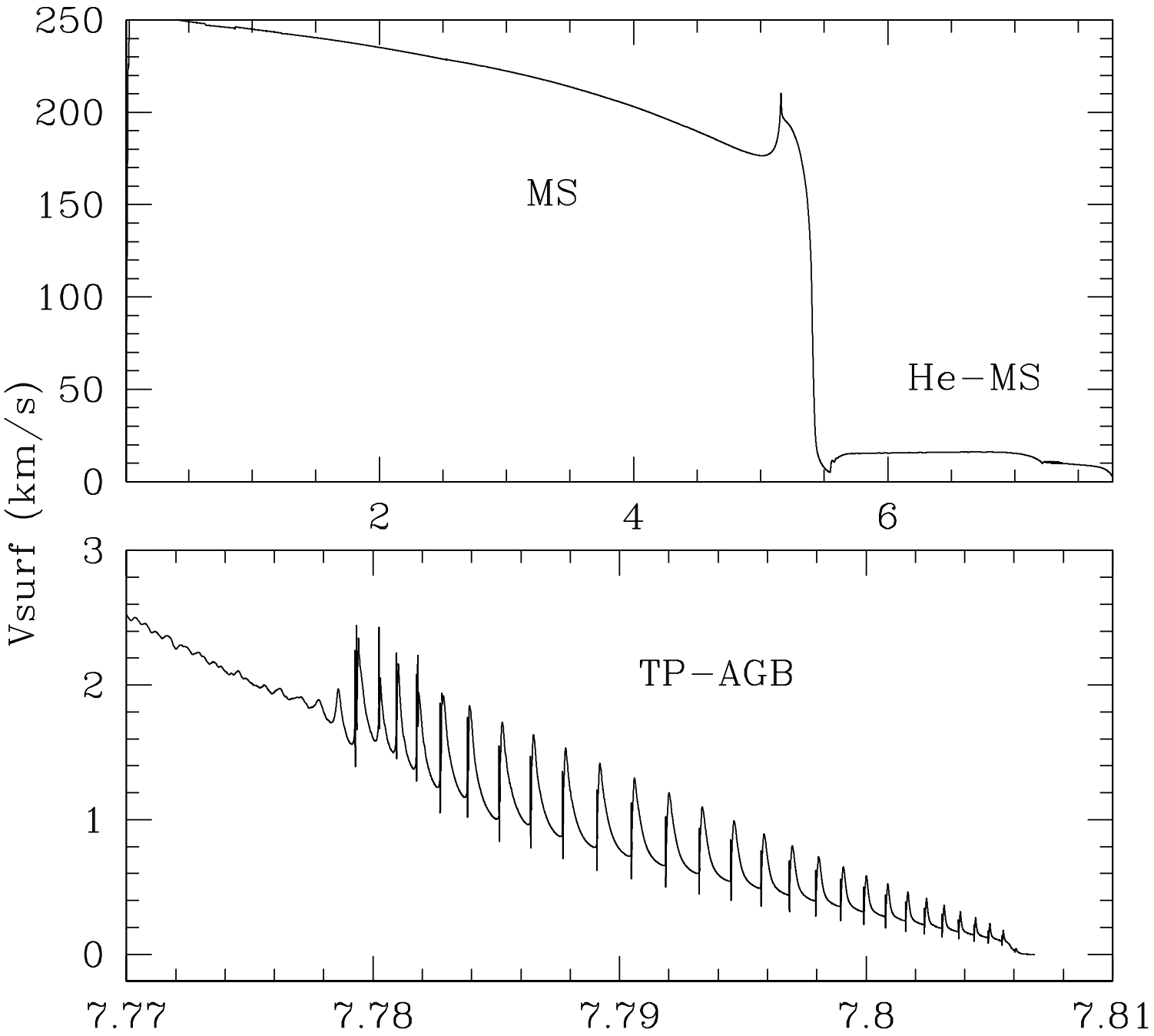

Fig. 2.— Evolution of the surface equatorial rotational velocity of the 2.5 $M_\odot$ model. The initial equatorial rotational velocity is 250 km s^{-1} and the model does not include magnetic torques. The top panel follows the evolution to the early TP-AGB phase and the bottom panel shows the rest of the evolution until the end of the calculation when the star reaches a temperature of 6400 K.

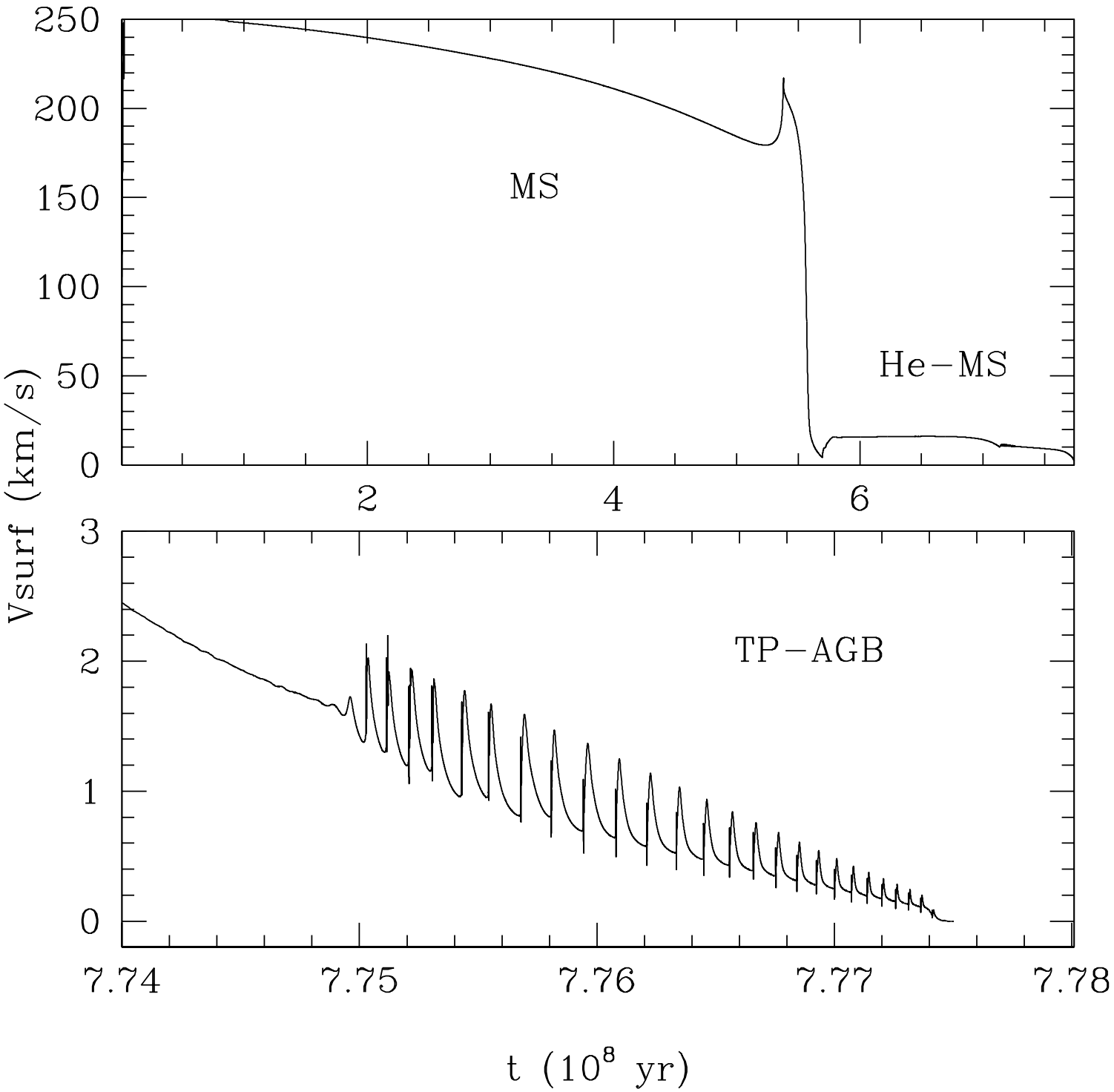

Fig. 3.— Same as Figure 2 but including angular momentum transport induced by magnetic torques.

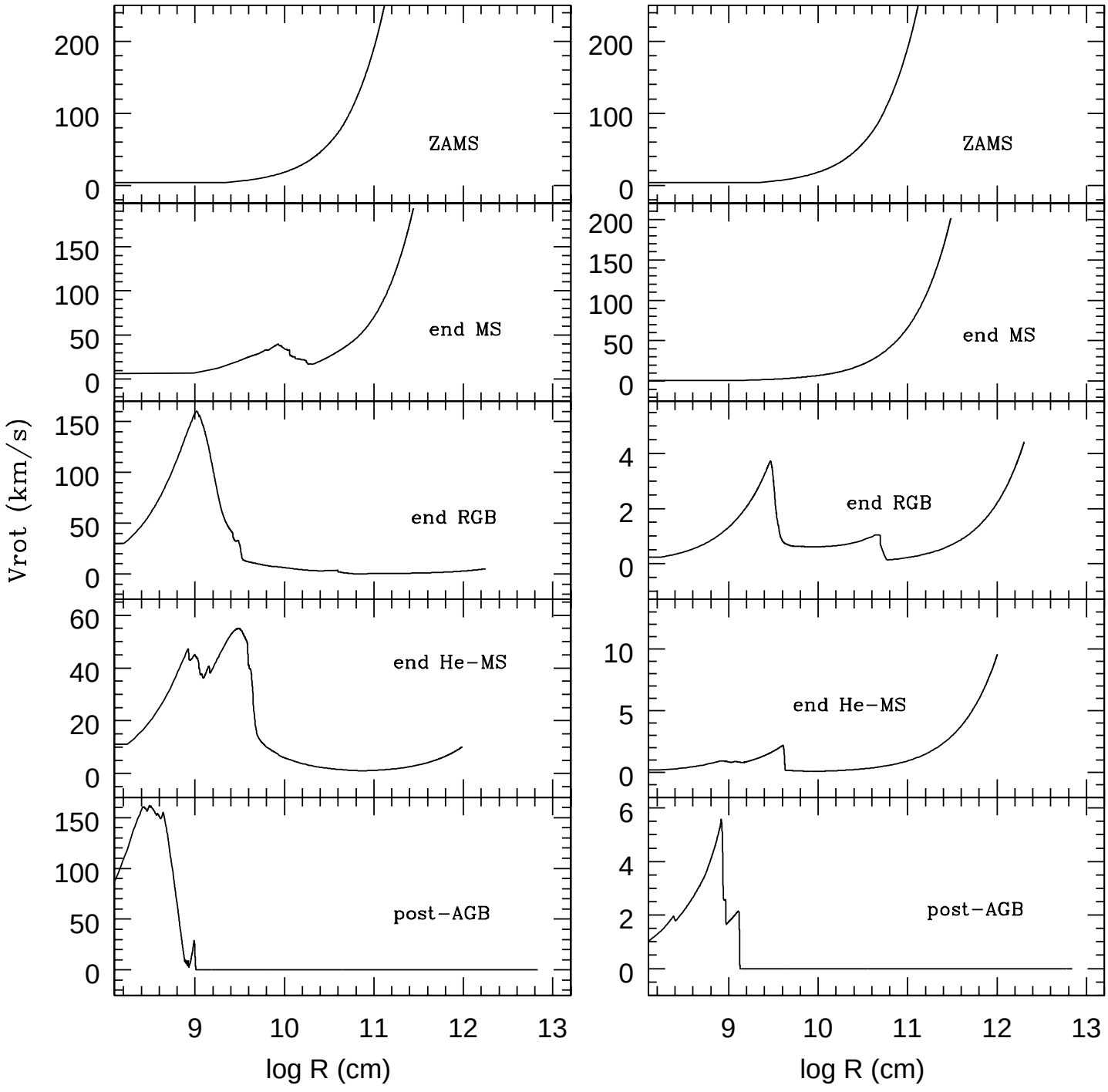

Fig. 4.— Snapshots of the distribution of the rotational velocities within the stellar structure taken at key evolutionary times. The non-magnetic case is in the left panels while the magnetic case in the right panels.

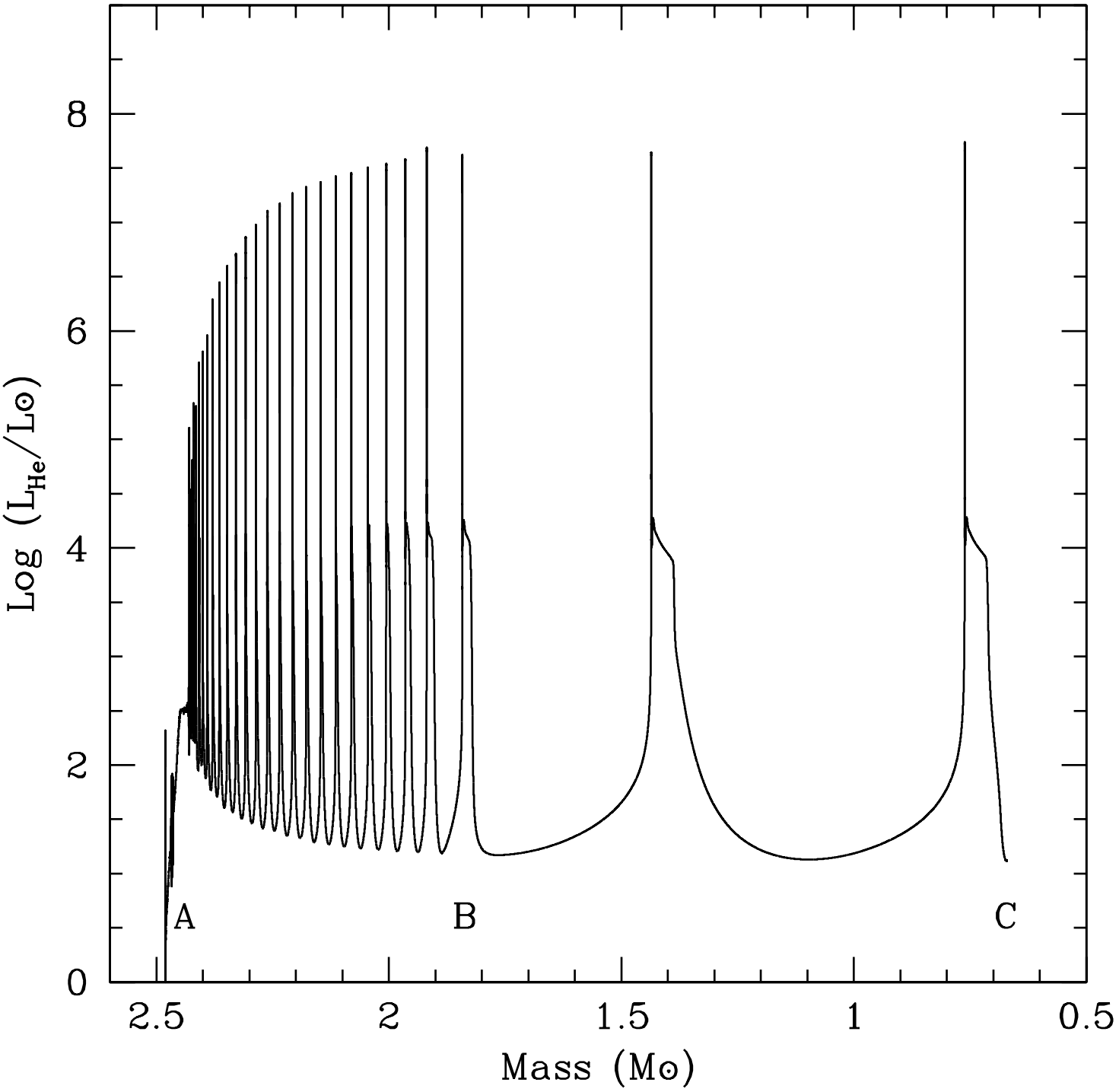

Fig. 5.— Evolution of the Helium burning luminosity as a function of the stellar mass.

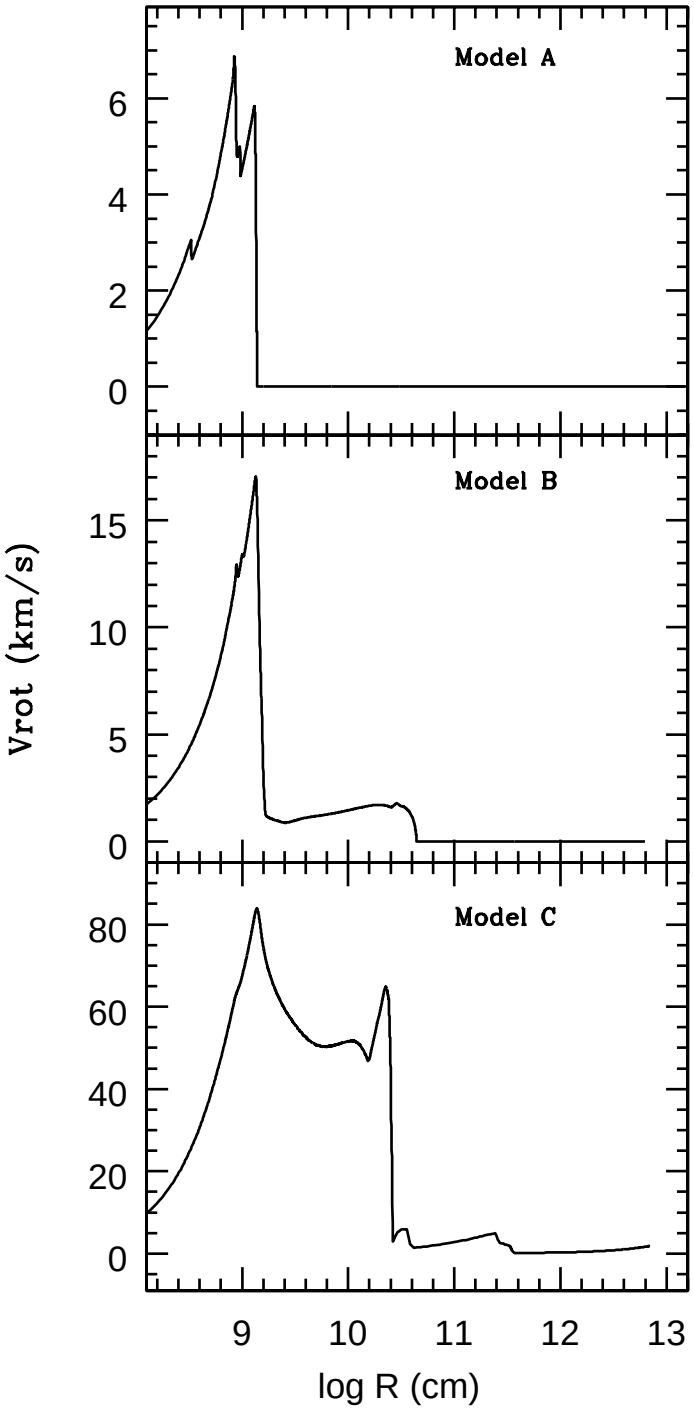

Fig. 6.— The distribution of the rotational velocities within the stellar structure at the post-AGB phase (6400 K).

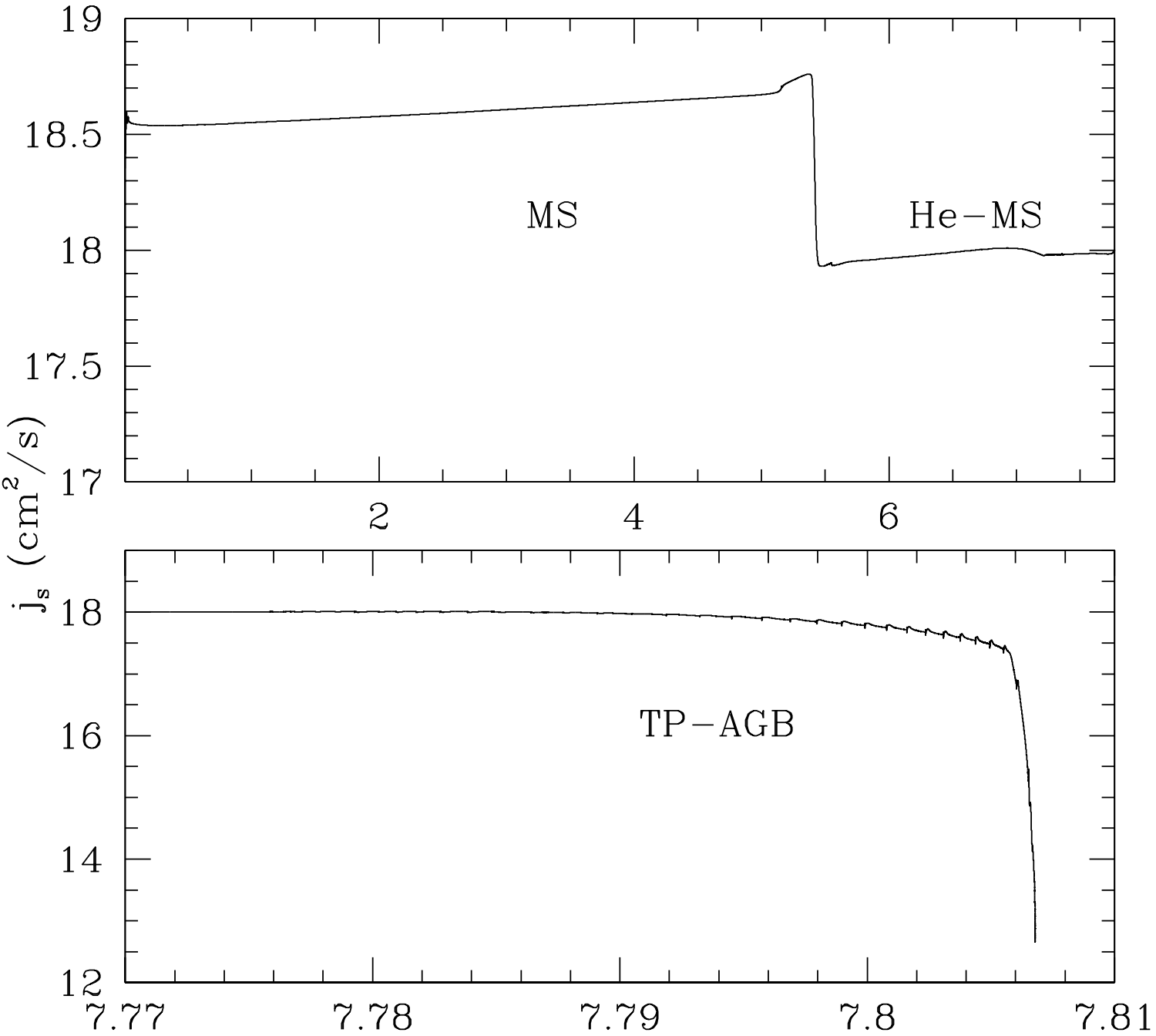

Fig. 7.— Evolution of the specific angular momentum of the surface layers for the 2.5 $M_\odot$ model without magnetic torques. The top panel follows the evolution to the early TP-AGB phase and the bottom panel shows the rest of the evolution until the end of the calculation when the star reaches a temperature of 6400 K.

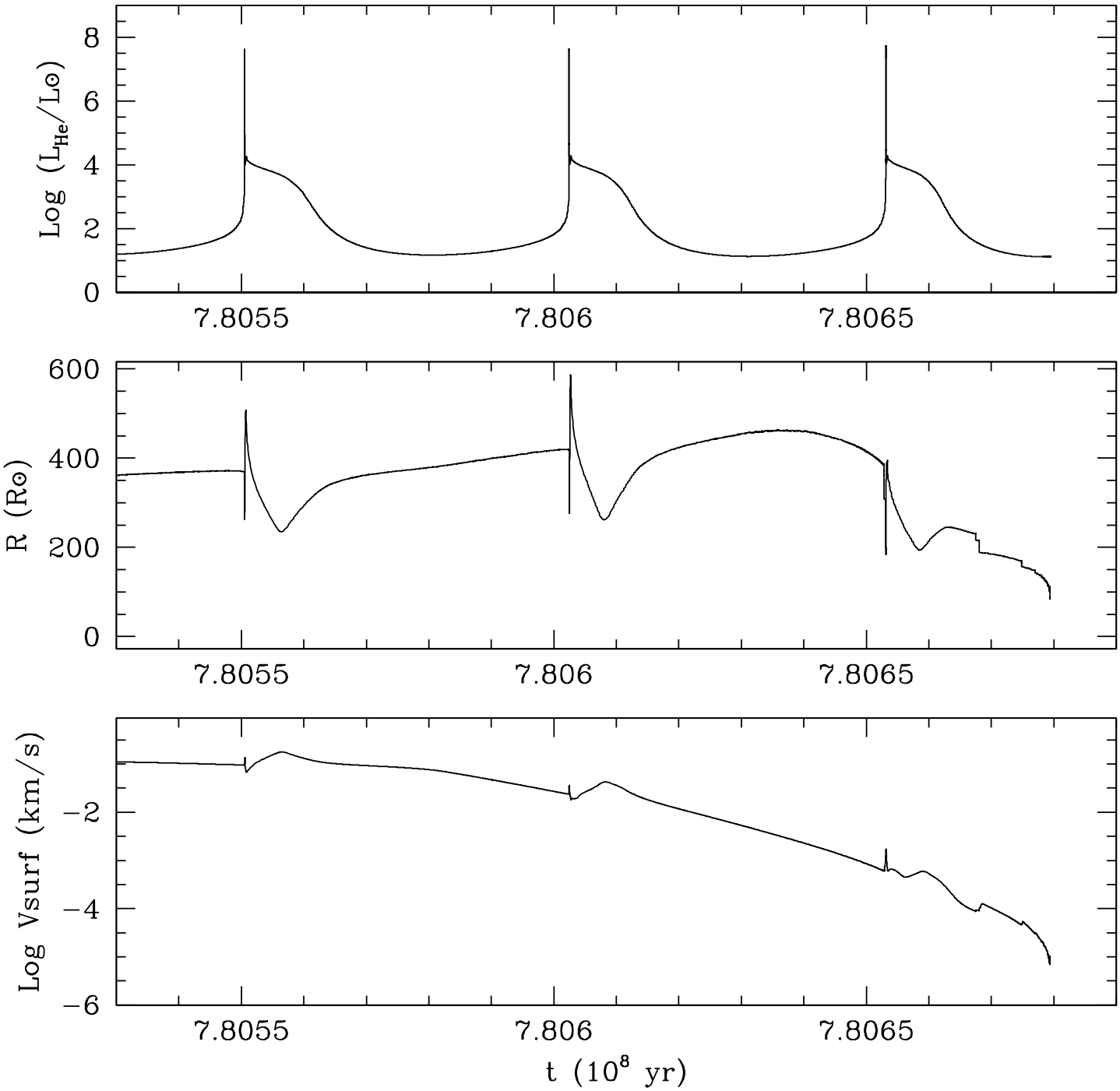

Fig. 8.— Evolution of the stellar radius (middle) and the surface rotational velocity (bottom) during the last three thermal pulses, which are shown on the top as the Helium luminosity. The last points correspond with the post-AGB at 6400 K .